JOURNAL OF MATERIALS SCIENCE 00 (1980) 2376–2384

Defect structure and tetrahedral precipitates in sulphur-doped gallium phosphide

R. K. BALL, P. W. HUTCHINSON
Department of Physical Metallurgy and Science of Materials, University of Birmingham, P.O. Box 363, Birmingham, UK

Transmission electron microscopy has been used to study the defect structure in liquid encapsulated Czochralski GaP doped with 2×10^{18} S atoms cm^{-3}. Dislocation clusters, stacking faults and precipitates were observed and analysed in as-grown, annealed and zinc diffused materials. In as-grown and annealed GaP both the perfect and faulted dislocation loops were shown to be interstitial in nature while the precipitates were found to be incoherent and tetrahedral in shape. Prolonged zinc diffusion was shown to increase the dislocation density and cause the precipitates to become coherent.

1. Introduction

Liquid encapsulated Czochralski (LEC) grown GaP is often used as a substrate material when fabricating light emitting diodes (LED). In order to improve device efficiency it is important that crystalline defects should be identified and characterized. It has already been demonstrated that climbing dislocation structures are responsible for rapid non-homogeneous degradation which arises during the operation of GaAs–GaAlAs lasers [1, 2], and that a similar dislocation structure may be responsible for the slow, bulk electroluminescence degradation which occurs in green GaP LEDs [3].

Recent transmission electron microscopy studies of GaP substrate materials have revealed the presence of three principal types of defects. These are: (a) Frank loops containing stacking faults, reported as intrinsic in nature by Umeno *et al.* [4] and as extrinsic in nature by Dupuy and Lafeuille [5] and Gibb and Augustus [6]; (b) perfect dislocation loops, given as vacancy in character by Stacy and de Kock [7], and as interstitial by Umeno *et al.* [4] and by Dupuy and Lafeuille [5], and (c) small precipitates of unknown chemical composition [4, 5, 7].

In the present work transmission electron microscopy has been employed to study the defect structure occurring in heavily S–doped GaP LEC substrate material. The effects of vacuum annealing and zinc diffusion on the defect structure have also been investigated.

2. Experimental procedure

The LEC GaP crystals were grown by Metals Research Ltd. (Royston). 0.3 mm thick slices, containing approximately 2×10^{18} electrically active sulphur atoms per cm^3, were cut from the crystal perpendicular to its ⟨0 1 5⟩ growth axis, mechanically lapped and chemically polished.

Zinc diffusions employing elemental zinc (99.9999% purity) and vacuum anneals (pressure $< 10^{-5}$ torr) were performed on such discs in sealed vitreosil quartz tubes. The approximate dimensions of the tubes were 5 cm length and 6 mm internal diameter.

Planar transmission electron microscope (TEM) specimens were prepared by chemically etching both faces using a saturated solution of chlorine in methyl alcohol, and transverse specimens were made from the zinc diffused samples using the method outlined by Abrahams and Buiocchi [8] and employing argon ion beam machining. The specimens were examined in both a high voltage AEI EM7 electron microscope and in a Philips EM400 microscope fitted with energy dispersive X-ray microanalysis facilities.

0022–2461/80/092376–09$02.90/0

3. Results

3.1. As-grown material

The principal defect structure of the as-grown material consisted of dislocation clusters comprising dislocation lines, helices and loops and colonies of precipitates whose sizes and distributions did not vary significantly across a slice. Fig. 1 shows a typical dislocation cluster. The general morphology of the dislocation clusters suggests that the dislocation lines may be parts of large, irregular

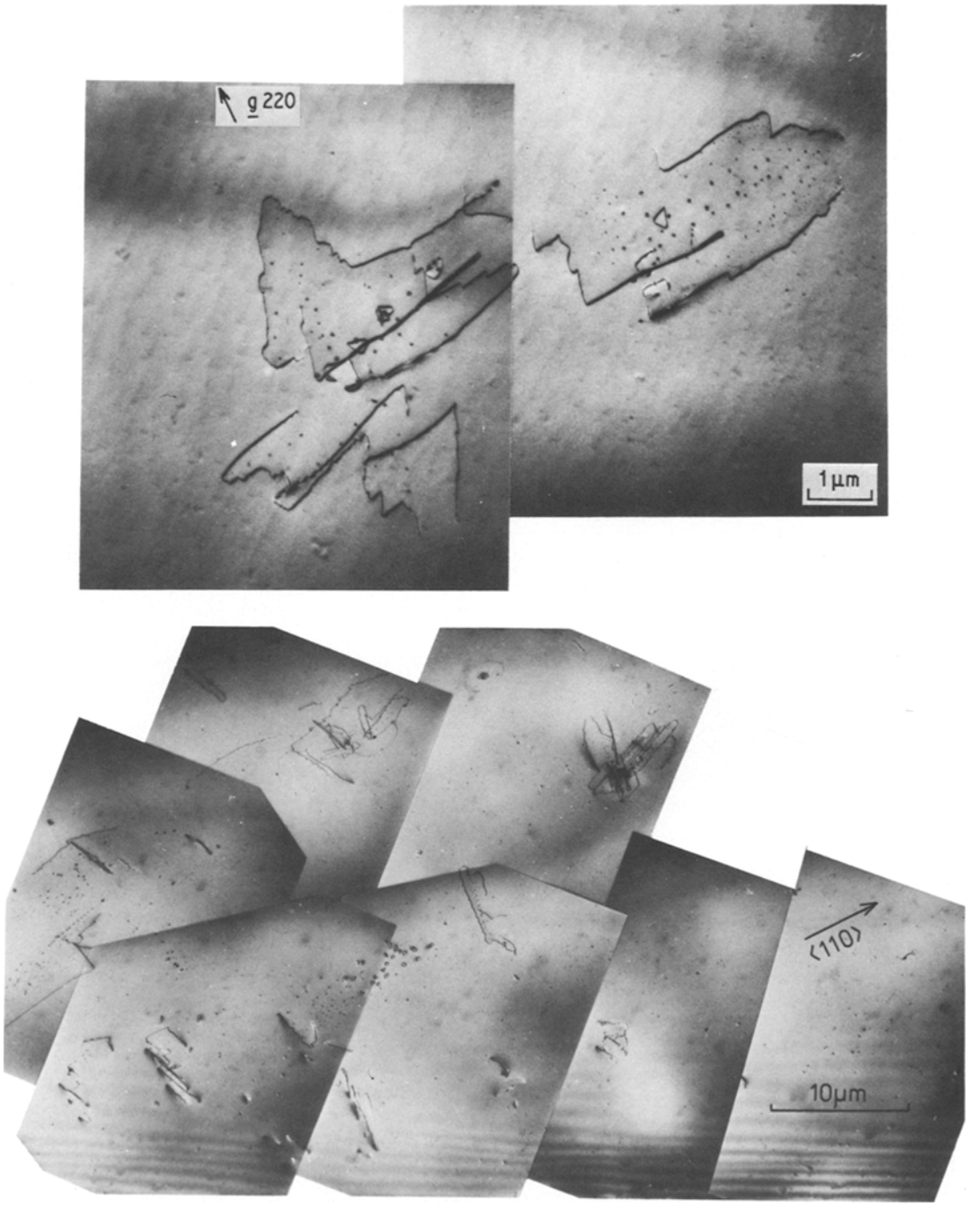

Figure 1 (a) Dislocation cluster and associated precipitate particles in as-grown sulphur doped gallium phosphide. B near [0 0 1], g 2 2 0. (800 kV.) (b) Low magnification TEM montage of as-grown GaP(S) showing the irregular nature and distribution of defect clusters. (800 kV.)

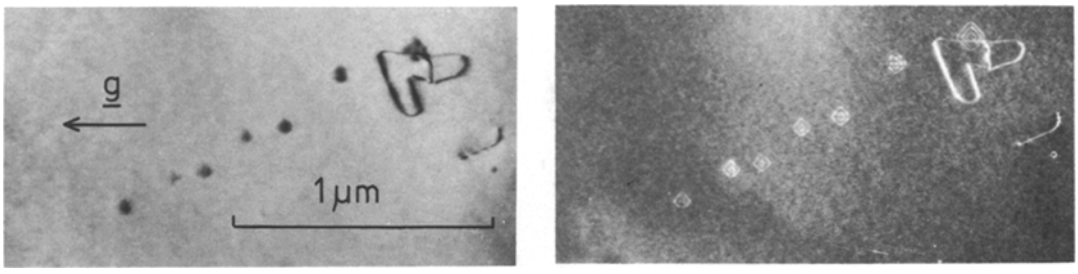

Figure 2 Precipitate particles in a specimen of as-grown material are revealed as squares in the (0 0 1) projection (a) bright field image, g 2 2 0; (b) weak beam dark field image, g 2 2 0 ($S_g \approx 0.0028$ Å^{-1}). (800 kV.)

shaped loops, of up to 10 μm across, whose extremities have been removed during thin foil preparation. Their similarity to the much smaller, irregular polygonal shaped loops reported in the earlier literature [4, 5, 9], and the distribution of the precipitate colonies supports this hypothesis. Because of the irregular shapes and the inhomogeneous distribution of the clusters (Fig. 1b) it was impossible to estimate their densities.

Faulted dislocation loops, with an average diameter of approximately 2 μm were also present with a non-uniform distribution but a lower density than the dislocation clusters. These were also usually accompanied by several precipitate particles. Those faulted loops intersecting the foil surfaces were analysed by the method of Gevers *et al.* [10] and were found to be extrinsic in nature.

Analysis of the dislocation structure within the clusters was also carried out. The dislocation lines were found, using the invisibility criteria, to have burgers vectors of $\frac{a}{2}\langle 1\,1\,0\rangle$, while, following the conventions and procedures outlined by Maher and Eyre [11], the loops were deduced as perfect, near edge, $\frac{a}{2}\langle 1\,1\,0\rangle$, interstitial defects, whose habit planes were intermediate between $\{1\,1\,0\}$ and $\{1\,1\,1\}$.

The precipitate particles were generally observed to occur only within the dislocation clusters and stacking faults, as Fig. 1b illustrates. Tilting experiments demonstrated that the particles lie adjacent to, or occasionally on, the dislocation extra half planes.

Detailed examination at high magnification revealed that they are all approximately tetrahedral in shape with average edge length 500 Å. Fig. 2 shows a typical bright field micrograph and a weak beam dark field micrograph of the same area, both taken with a beam direction close to [0 0 1]. Although the morphology is not clear in the bright field micrograph, the weak beam micrograph clearly illustrates that the particles appear as squares when viewed along this direction. After tilting to a $\langle 1\,1\,2\rangle$ beam direction, however, the defects are seen as triangles. Fig. 3 shows the bright field and weak beam images of such defects in an annealed specimen. Similarly when employing a $\langle 1\,1\,0\rangle$ beam direction the defects once again appear triangular. Thus it is concluded that they are tetrahedral in shape with $\{1\,1\,1\}$ facets. Fig. 4 indicates that all the tetrahedra have equivalent crystallographic orientations. However, it was noted that with increasing size the tetrahedral shape was lost as the vertices became truncated. (Fig. 5). The possibility that they may be tetrahedral stacking faults was eliminated by considering the fringe contrast observed in matrix weak beam mode. As Figs. 2, 3, 4, and 6 demonstrate

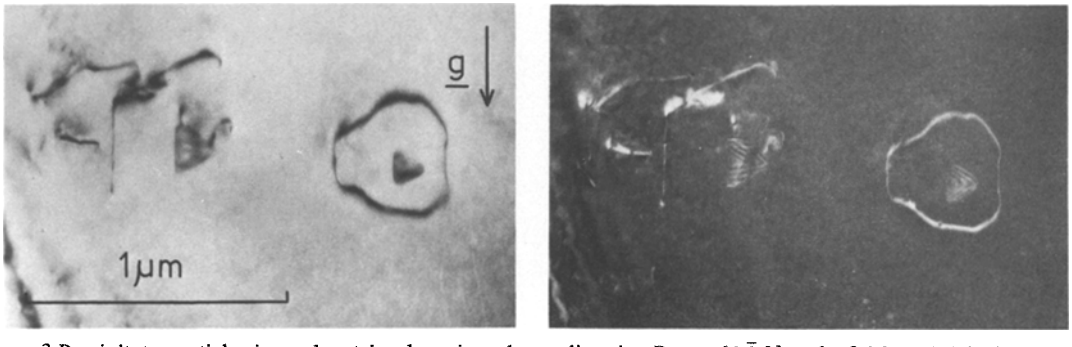

Figure 3 Precipitate particles imaged as triangles using a beam direction B near $[1\,\bar{1}\,2]$ and g 2 2 0 (a) bright field image (b) weak beam dark field image. (800 kV.)

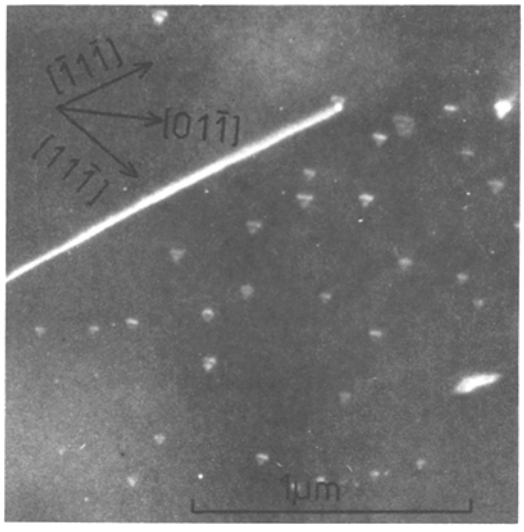

Figure 4 A cluster of precipitate particles imaged with B [0 1 1] and g 1 1 $\bar{1}$ showing that all the tetrahedra have equivalent crystallographic orientations. Area from a transverse specimen, sample annealed at 850° C for 1.5 h, foil normal N ≈ 112. (800 kV, $S_g \approx 0.011$ Å^{-1}).

the contrast is consistent with the thickness fringes of a tetrahedral void but not with the stacking fault fringes expected from a faulted tetrahedron.

The bright field image contrast varied from defect to defect and also varied across each individual defect. However, in general, a brighter region could be observed within the defects and this is a phenomenon which becomes more evident with increasing size of the defects. (Fig. 5). A similar effect has been observed in precipitates in GaAs [12] and from this it is tentatively deduced that they are, in fact, precipitates containing a small void. Several of the particles in the thinnest region of the foils were examined with the EDAX facility but, apart from gallium and phosphorus, no other X-ray signals were detected. Attempts to identify these defects from microdiffraction patterns were also unsuccessful.

An interesting observation which is not completely understood is that a change in contrast of the precipitates is observed during the first few seconds of exposure to a fully condensed electron beam (as Fig. 7 illustrates). Careful tilting experiments failed to reproduce the originally observed contrast and thus it is deduced that a change in diffraction conditions under the heating effects of the electron beam is not responsible. There is, however, a possibility that the change may be due to the elimination of strain contrast.

3.2. Vacuum annealed material

During device fabrication GaP substates may be subjected to elevated temperatures, between 650 and 1050° C, for several hours. The effects of heat treatments on the defect structures were investigated by a series of vacuum annealing experiments. Four separate annealing treatments were used: (a) 925° C for 24 h, (b) 850° C for 3 h, (c) 850° C for 24 h and (d) 625° C for 168 h. In each case the defect structures were similar to those observed in the as-grown materials.

While there was no detectable difference between the defect structure of specimens (b) and as-grown materials, in (a), (c) and (d) there was a

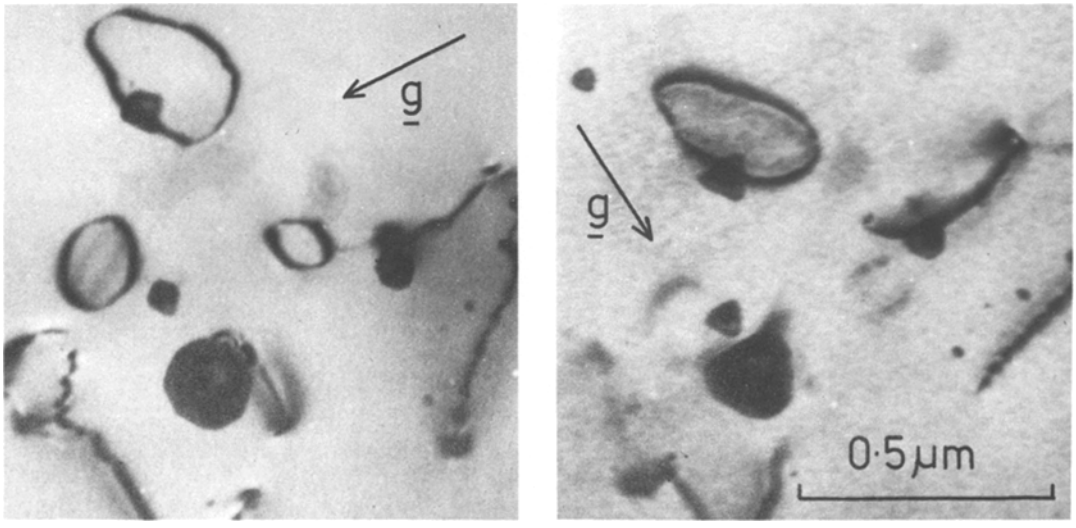

Figure 5 A truncated precipitate in an annealed (at 625° C for 168 h) specimen (100 kV), (a) B ~ [0 0 1], g 2 2 0; (b) B ~ [1 $\bar{1}$ 2], g $\bar{1}$ 1 1.

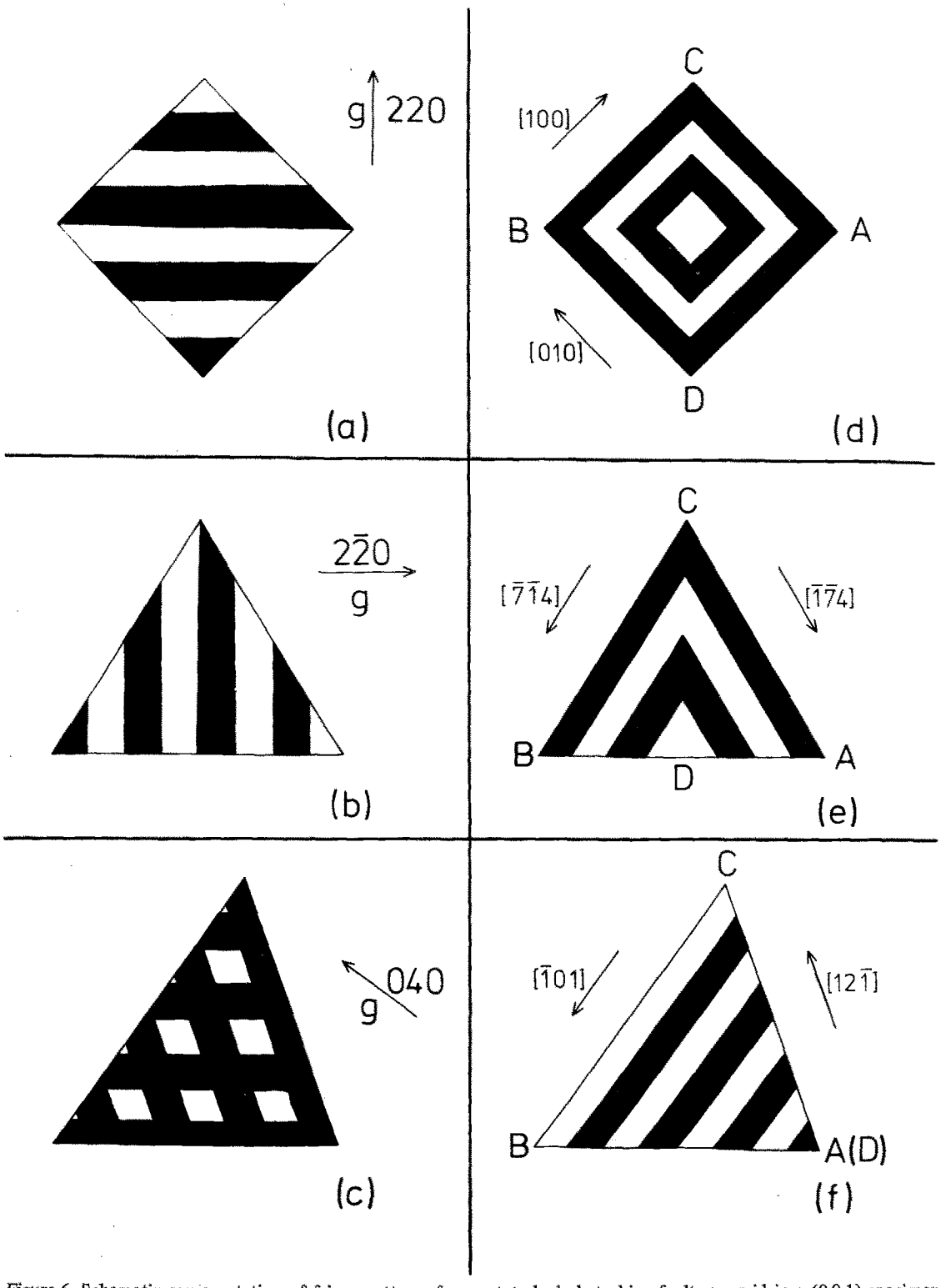

Figure 6 Schematic representation of fringe patterns from a tetrahedral stacking fault pyramid in a (0 0 1) specimen, (a) g 2 2 0, b 0 0 1; (b) g 2$\bar{2}$0, b [1 1 2]; (c) g 0 4 0; b [1 0 1] and equal thickness fringes from a tetrahedral void or precipitate in a parallel-sided foil with (d) b [0 0 1], (e) b [1 1 2] and (f) b [1 0 1].

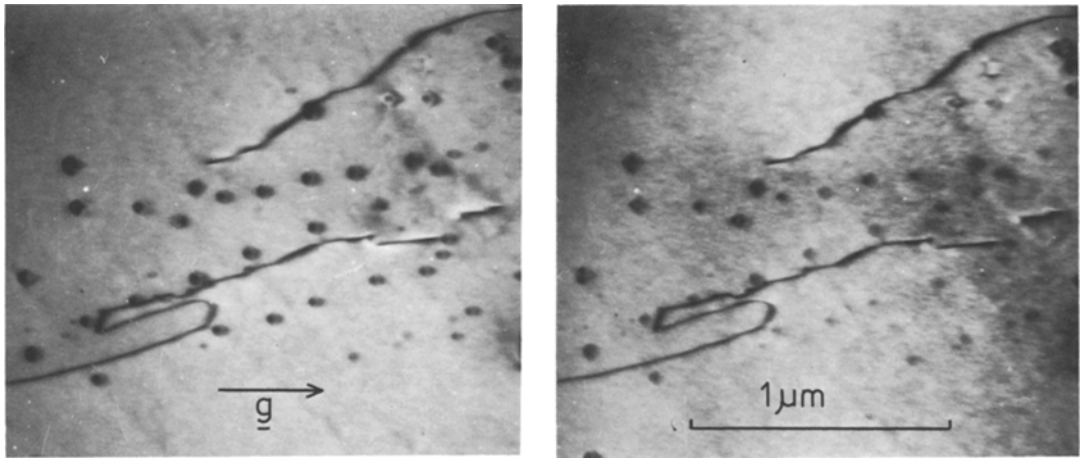

Figure 7 Bright field micrographs of specimen with **B** ~ [0 0 1] and g 2 2 0, taken with a decondensed beam, illustrating the effects of a condensed electron beam on the contrast observed at precipitate particles, (a) initially and (b) after about 20 seconds exposure to a condensed beam. (800 kV.)

slight increase in perfect loop density *within* the clusters. Such loops were associated with the precipitates, this being most noticeable where rows of precipitates were accompanied by rows of loops. The precipitates appeared to lie adjacent to, but not in, the plane of the loops as is demonstrated in Fig. 8 where loop A, and its accompanying precipitate is shown edge on.

Analysis of the perfect and faulted loops indicated that they were interstitial and extrinsic in nature respectively similar to those observed in the as-grown material.

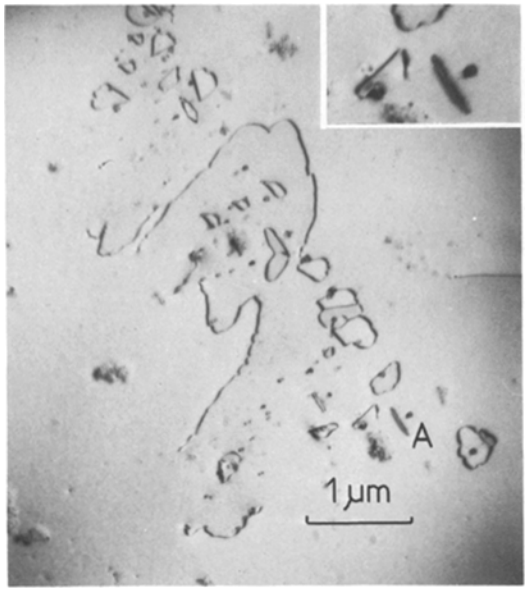

Figure 8 Dislocation cluster in specimen, vacuum annealed at 962° C for 24 h, with **B** ~ [0 0 1] and g $\bar{2}$ 2 0, showing an increase in perfect loop density. The inset shows loop A and accompanying precipitate at higher magnification. (800 kV.)

3.3. Zinc diffusion

Zinc diffusions were carried out at 850° C for 3 hours and for 24 hours in order to accord a direct comparison with the annealing experiments.

Planar TEM specimens, diffused for 3 hours and thinned to within the diffused zone, revealed the presence of dislocation clusters and faulted dislocation loops whose sizes, densities and distribution showed little difference from those observed in the specimens annealed under similar conditions. Once again precipitates were observed in conjunction with the dislocation structures, but these precipitates exhibited strain contrast effects, as shown in Fig. 9, which suggests that they are coherent. Transverse specimens were also examined and these too confirmed that the defect distributions, densities and sizes were similar in both the zinc-diffused and annealed-only regions. The examinations also showed that the precipitates were coherent in the diffused zone but were tretrahedral and incoherent in the annealed region.

However, planar specimens diffused for 24 hours, and examined in the diffused region, while showing all the features of the short time diffusion, also contained a high density of dislocation loops, precipitates and lines *between* the original clusters. These results suggest that there may be an incubation period, such as has been found in GaAs [13], which it is necessary to exceed before diffusion induced defects can result.

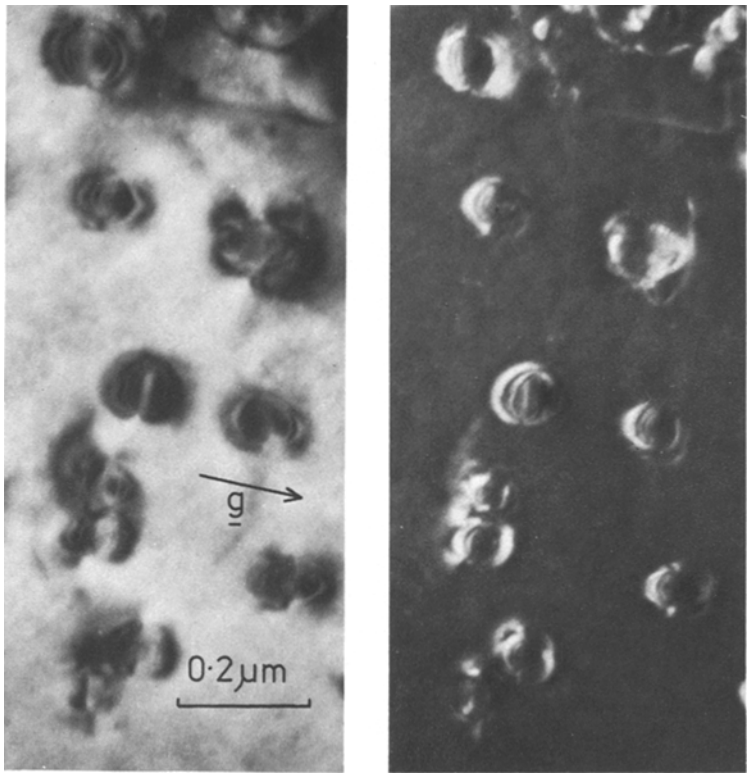

Figure 9 Precipitates in Zn-diffused GaP (S) (annealed at 850° C for 3 h) exhibiting strain contrast with **B** ~ [0 0 1] and g 2 2 0, (a) bright field and (b) weak beam dark field image. (800 kV.)

Examination of the coherent precipitates with EDAX indicated the presence of zinc.

4. Discussion

The defect structure observed in the as-grown material has probably developed during cooling of the pulled crystal. Since the dislocation structure and precipitates are always present together, and in isolated clusters, then by implication one must be the consequence of the other.

Umeno *et al.* [4], have proposed a dislocation loop growth process (similar to that given for NbC precipitation in austenitic stainless steels by Silcock and Tunstall [14]) whereby excess sulphur precipitates and the subsequent growth induced stresses are relieved by the simultaneous climb of an associated dislocation loop. Large polygonal loops containing colonies of precipitates result as further precipitate nucleation and growth, and climb of the loops, occurs. EDAX investigations carried out in this work have, however, failed to identify the presence of sulphur within the particles and the above model must, therefore, be modified with the contaminants O, B, or C, or even excess Ga or P taking the place of the sulphur.

The inhomogeneous distribution of faulted loops, whereby their random distribution was occasionally interrupted by a region of comparatively high density, showed some similarity to the results of Kamejima *et al.* [15] which indicated that stacking faults in S-doped GaAs occurred predominantly in regions of sulphur segregation. Thus the stacking faults in both materials may consist of $\{1\,1\,1\}$ layers of Ga_2S_3 and be similar in structure to the $\{1\,1\,1\}$ layers of Ga_2Te_3 proposed by Hutchinson and Dobson [16] in Te-doped GaAs. Alternatively, the co-existence of stacking faults and precipitates may suggest a nucleation process similar to that described for the dislocation loops and clusters.

The similarity between as-received and annealed specimens indicates that the temperatures used during device fabrication will not adversely affect the defect structure since the slight increase in loop density within the clusters only occurs after prolonged annealing. Since such loops are always located near the precipitates, and considering the position of the precipitates (Fig. 8), then it is probable that they have been generated by a "punching out" mechanism and subsequently climbed, as suggested by Umeno *et al.* [4]. This process is expected to be slow, as shown by the annealing results, since the surrounding dislocation tangles will act as a sink for point defects.

An alternative to this process arises from the observation that many of the dislocation lines within the clusters exhibited helical coils and were accompanied by rows of loops, a situation similar to that reported by Dupuy and Lafeuille [5]. Such coils may therefore, as suggested by these authors, climb and pinch-off to give a row of loops. The results of the present work, however, have shown that most of the loops in such a row have different burgers vectors from the adjacent helix, which suggests that, although this process may occur, it is a second order mechanism as compared with that described by Umeno *et al.* [4]. The fact that the loops in the as-grown and annealed materials are both interstitial and associated with precipitates implies a similar nucleation process. This, combined with the interstitial nature of the polygonal loops [4] observed in less heavily S-doped materials, suggests that the same dislocation generation process, i.e. the punching out of loops from precipitates, is common to all.

Analysis of faulted loops showed that they are extrinsic in both as-grown and annealed GaP; and since they occur in both materials with similar sizes, shapes, and densities it is tentatively concluded that the stacking faults developed during crystal growth and remained unchanged during the annealing treatments employed in this work. These results therefore disagree with the conclusions of Umeno *et al.* [4], who gave the fault nature in as-grown material as intrinsic, and explained the difference between their results and those of Dupuy and Lafeuille [5], who reported extrinsic faults in their fabricated substrates, as being due to the different thermal histories of their specimens.

The dislocation structure observed in a specimen after a 3 hour zinc diffusion was found to be the same as that seen in as-grown and 3 hour annealed specimens in accordance with the results of Dupuy and Lafeuille [5]. The fact that the precipitates exhibit a strain field in the diffused region and that EDAX observations indicate zinc within the precipitates suggests that zinc has either reacted with, or been incorporated into, the original tetrahedral precipitates, and the resultant growth has produced stresses between the particles and the matrix. The presence of additional dislocations and precipitation after prolonged zinc diffusion is in accordance with the idea that an incubation period is necessary before the production of diffusion induced defects occurs.

The failure of EDAX techniques to detect sulphur in the precipitates is not altogether surprising, since small precipitates have also been reported in undoped GaP [9]. Small precipitates have also been observed in semi-insulating, n-type and p-type GaAs and EDAX analysis has also failed to identify the chemical constituents of these precipitates [17]. Since small precipitates occur in such a wide variety of GaAs and GaP material, and since EDAX measurements fail to register the presence of intentionally added impurity dopants, the most likely candidates for precipitation are either excess matrix elements, or contaminants such as oxygen, boron, and carbon, which EDAX observations are incapable of detecting.

Cullis *et al.* [12], have recently identified small precipitates in Cr-doped GaAs as arsenic from selected area diffraction. Although we have been unable to obtain any microdiffraction from the precipitates in GaP it is quite possible that these contain P (or Ga) by analogy with the GaAs, since the two materials are closely related and the growth procedures are similar.

As previously noted, all of the tetrahedral precipitates have equivalent crystallographic orientations, that is they are all bounded by facets on only one of the two sets of $\{1\,1\,1\}$ matrix planes: either Ga $(1\,1\,1)$, $(\bar{1}\,\bar{1}\,1)$, $(\bar{1}\,1\,\bar{1})$, $(1\,\bar{1}\,\bar{1})$ or P $(\bar{1}\,\bar{1}\,\bar{1})$, $(1\,1\,\bar{1})$, $(1\,\bar{1}\,1)$, $(\bar{1}\,1\,1)$, although which set is applicable has not yet been determined.

Such examples of asymmetry are common in the III–$\overline{\text{V}}$ compounds which crystallize with the zinc-blende structure.

5. Conclusions

(1) Extrinsic faults and dislocation clusters are present in as-grown GaP in conjunction with small incoherent tetrahedral precipitates.

(2) The heat-treatments typically employed during device processing do not significantly affect the defect structures, though prolonged annealing does increase the number of interstitial dislocation loops within the clusters through a "punching out" mechanism around precipitates.

(3) Although zinc diffusion causes the precipitates to become coherent, no significant changes in dislocation structure are apparent unless long diffusion times are employed.

(4) The chemical composition of the tetrahedral precipitates has not been identified but it is possible that they contain either contaminants such as O, B or C or one of the matrix elements Ga or P.

(5) The tetrahedral particles all have the same crystallographic orientations and therefore reflect the polarity of the zinc-blende *lattice* of the matrix.

Acknowledgements

The authors acknowledge financial support from the Science Research Council. We are grateful to Professor R. E. Smallman and Dr. P. S. Dobson for the provision of laboratory facilities and to Dr. M. H. Loretto and Dr. I. P. Jones for assistance with the EDAX facility and for useful discussions.

References

1. P. PETROFF and R. L. HARTMAN, *Appl. Phys. Lett.* **23** (1973) 469.
2. P. W. HUTCHINSON, P. S. DOBSON, S. O'HARA and D. H. NEWMAN, *ibid.* **26** (1975) 250.
3. P. M. PETROFF, O. G. LORIMOR and J. M. RALSTON, *J. Appl. Phys.* **47** (1976) 1583.
4. M. UMENO, H. KAWABE and K. DOI, *Phil. Mag.* **39** (1979) 183.
5. M. DUPUY and D. LAFEUILLE, *J. Cryst. Growth* **31** (1975) 244.
6. R. M. GIBB and P. D. AUGUSTUS, *J. Elect. Mater.* **5** (1976) 585.
7. W. T. STACY and A. J. R. DE KOCK, *ibid.* 7 (1978) 705.
8. M. S. ABRAHAMS and C. J. BUIOCCHI, *J. Appl. Phys.* **45** (1974) 3315.
9. A. J. R. DE KOCK, W. M. VAN DE WIJGERT, J. H. T. HENGST, P. J. ROKSNOER and J. M. P. L. HUYGBRETS, *J. Cryst. Growth* **41** (1977) 13.
10. R. GEVERS, A. ART and S. AMELINCKX, *Phys. Stat. Sol.* **3** (1963) 1563.
11. D. M. MAHER and B. L. EYRE, *Phil. Mag.* **23** (1971) 409.
12. A. G. CULLIS, P. D. AUGUSTUS and D. J. STIRLAND, *J. Appl. Phys.*, to be published.
13. J. F. BLACK and E. D. JUNGBLUTH, *J. Electrochem. Soc.* **114** (1967) 188.
14. J. M. SILCOCK and W. J. TUNSTALL, *Phil. Mag.* **10** (1964) 361.
15. T. KAMEJIMA, J. MATSUI, Y. SEKI and H. WATANABE, *J. Appl. Phys.* **50** (1979) 3312.
16. P. W. HUTCHINSON and P. S. DOBSON, *Phil. Mag.* **30** (1974) 65.
17. P. D. AUGUSTUS and D. J. STIRLAND, *J. Microscopy* **118** (1980) 111.

Received 7 February and accepted 3 March 1980.